



The Effects of Humidity on Spontaneous Cocrystallization: A Survey of Diacid Cocrystals with Caffeine, Theophylline, and Nicotinamide

Riley D. Davies¹ · Nicolas J. Vigilante¹ · Aaron D. Frederick¹ · Venkata S. Mandala¹ · Manish A. Mehta¹

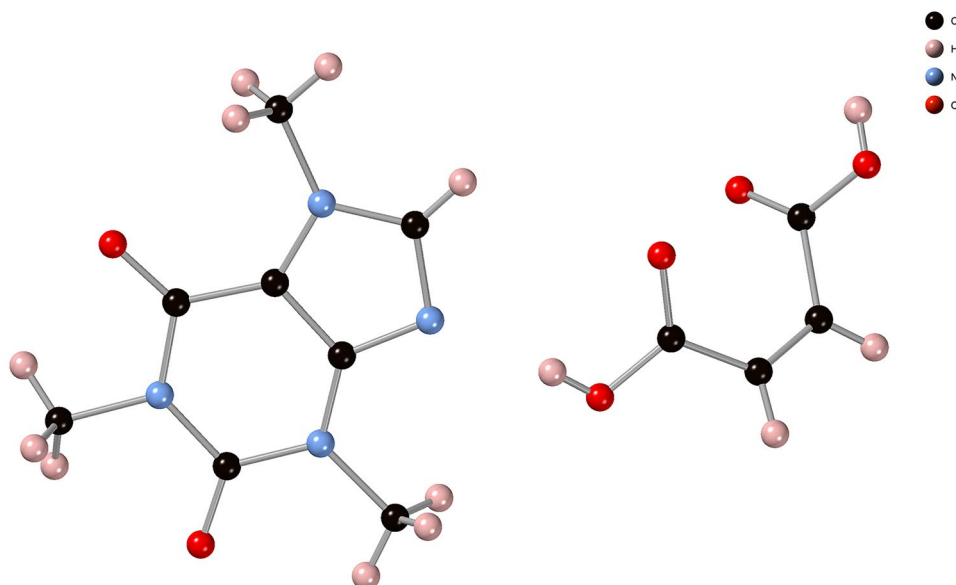
Received: 3 September 2021 / Accepted: 5 January 2022

© The Author(s), under exclusive licence to Springer Science+Business Media, LLC, part of Springer Nature 2022

Abstract

Pharmaceutical cocrystals comprise one active pharmaceutical ingredient (API) and at least one small molecule excipient coformer. While solvent evaporation and mechanochemistry are the preferred methods for their synthesis, some cocrystals are known to form spontaneously at ambient conditions when powders of input materials are mixed—a process not yet fully understood. Aqueous humidity is also known to accelerate spontaneous cocrystal formation. We report here the extent of spontaneous cocrystallization for 14 cocrystal systems, at four levels of humidity. The binary cocrystals in our study consist of a model API (caffeine, theophylline, nicotinamide) and a small chain diacid coformer (oxalic acid, malonic acid, maleic acid, fumaric acid, succinic acid, glutaric acid). The spontaneous cocrystal formation was monitored *ex situ* by powder X-ray diffraction over several weeks. Our results show cocrystal formation in all 14 systems to varying extent and are consistent with literature reports that higher humidity correlates with more rapid cocrystal formation. We find that cocrystals containing smaller coformers often form faster. Based on our findings, we identify several cocrystals as candidates for future study.

Graphical Abstract



Keywords Cocrystal · Pharmaceutical · Powder X-ray diffraction · Humidity · Solid phase

✉ Manish A. Mehta
manish.mehta@oberlin.edu

¹ Department of Chemistry and Biochemistry, Oberlin College, 119 Woodland Street, Oberlin, OH 44074, USA

Abbreviations

CA Caffeine
TH Theophylline
NA Nicotinamide

| | |
|------|--------------------------|
| OA | Oxalic acid |
| MA | Malonic acid |
| ME | Maleic acid |
| FU | Fumaric acid |
| SU | Succinic acid |
| GA | Glutaric acid |
| PXRD | Powder X-ray diffraction |

Introduction

The study of cocrystals—multicomponent molecular crystals—is a burgeoning field in both materials and pharmaceuticals research [1, 2]. Several methods have proven effective in synthesizing cocrystals from solid-state molecular constituents. Two that provide the most consistent and effective results are precipitation via solvent evaporation and liquid-assisted mechanochemistry [1–6]. When applying solvent-based methods on an industrial scale, however, these techniques pose substantial environmental concerns [7, 8]. Solvent usage alone accounts for about 20% of all anthropogenic volatile organic compound (VOC) emissions. In the past 15 years, VOC emission reduction in industries other than fuel and transportation has stagnated [9, 10]. Development of solvent-free synthesis methods that rival the efficiency of current industrial approaches is thus an important step in reducing VOC emissions [7]. Mechanochemistry is one such green synthesis method [8, 11, 12], but another has recently gained attention: some cocrystals form spontaneously when powders of input materials are mixed, eliminating the need for energy input in grinding [7, 13–16]. Furthermore, solvent vapors, including aqueous humidity, are known to accelerate spontaneous cocrystallization in many systems [14–16]. The mechanism by which cofomers react in the solid state, as well as the catalytic role of solvent vapors, however, is not fully understood; however, there have been recent advances in understanding the role of vapor sorption and hygroscopicity in cocrystal formation [17–22]. Current research efforts to test the veracity of proposed transport mechanisms have not yet yielded a satisfactory kinetic model [23–26]. Additional data on the kinetics, molecular dynamics, and energetics of spontaneous cocrystallization are thus needed to establish a mechanism consistent with experimental evidence [18–22]. Here we present kinetics data for the spontaneous solid-state cocrystallization of fourteen different cocrystal systems at four humidity levels and we discuss trends in the data based on structure and experimental factors.

Experimental

We studied binary cocrystals that comprise of one of three model Active Pharmaceutical Ingredients, or APIs (Caffeine, CA; Theophylline, TH; Nicotinamide, NA) and one



Fig. 1 Chemical structures of the three model APIs used in this study

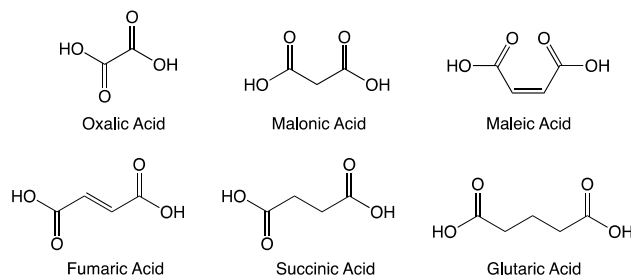


Fig. 2 Chemical structures of the six diacid cofomers used to form cocrystals with the APIs in Fig. 1

of six short chain diacids (Oxalic Acid, OA; Malonic Acid, MA; Maleic Acid, ME; Fumaric Acid, FU; Succinic Acid, SU; Glutaric Acid, GA). Chemical structures of the APIs are shown in Fig. 1 and those of the diacids cofomers are shown in Fig. 2. None of the cocrystals studied here are hydrates, which obviates complications arising from the incorporation of water into the crystal structure. All compounds were purchased from Sigma Aldrich, were reagent grade, and used without further purification. Each cocrystal's composition—both cofomers and stoichiometry—is presented in Table 1 in the format API:diacid. The stoichiometric ratios are the same as those reported in the literature [27–32]. Not all binary combinations form a cocrystal or were singled out for this study, although the structures of all 14 cocrystals studied here have been previously reported [27–32]. Six of the 14 cocrystals form in a 1:1 ratio, while the remaining eight form in a 2:1 ratio of API:diacid.

Powder X-Ray Diffraction (PXRD) was used to collect reference traces for all materials in Table 1 (individual cofomers and cocrystals) and to track all kinetics experiments. Data were collected on a RIGAKU Ultima IV diffractometer (Cu K α ; $\lambda = 1.581 \text{ \AA}$; 2θ sweep 5° – 40° , sweep speed $4^\circ/\text{min}$) using an aluminum sample holder. Reference cocrystals in Table 1 were made by mechanochemical means using a Retsch 400 MM ball mill (25-mL stainless steel jar, one stainless steel shot). Particle size of starting materials is known to influence the rate of spontaneous cocrystallization [16]. To allow for consistent data sets, input materials (API, cofomer) were manually sieved separately to collect powder fractions with 45–90 μm grain size. PXRD traces

Table 1 Cocrystal components and their stoichiometric ratios, with the model API given in the first column and the diacid cofomer given in the first row. Cocrystals not included in this study or cocrystals that do not form are marked with an X in the appropriate entry

| | Oxalic Acid (OA) | Malonic Acid (MA) | Maleic Acid (ME) | Fumaric Acid (FU) | Succinic Acid (SU) | Glutaric Acid (GA) |
|-------------------|------------------|-------------------|------------------|-------------------|--------------------|--------------------|
| Caffeine (CA) | 2:1 | 2:1 | 1:1 2:1 | X | X | 2:1 |
| Theophylline (TH) | 2:1 | 1:1 | 1:1 | X | X | 1:1 |
| Nicotinamide (NA) | 2:1 | 2:1 | X | 1:1 | 2:1 | 1:1 |

of all cofomers and cocrystals are provided in the Supplementary Information.

Previous work has shown that the presence of solvent vapors, including water vapor, can enhance the rate of cocrystallization in some systems—a process sometimes referred to as accelerated aging or vapor digestion [14, 33]. In this study, we set out to survey the effect of humidity by tracking cocrystal formation kinetics over a long period of several weeks. Spontaneous cocrystallization experiments were conducted at room temperature at four levels of relative humidity (RH) for each cocrystal system: 0% RH, 50% RH, 75% RH, and ambient laboratory conditions. A 0% RH environment was created in a 500-mL glass jar with a layer of calcium sulfate desiccant on the bottom. The jar with the desiccant was heated for 24 h in a drying oven prior to use. A 50% RH environment was created in a 500-mL glass jar using a saturated calcium chloride solution on the bottom, and a 75% RH environment was created using a saturated sodium chloride solution. The jars were sealed with a threaded lid. Samples were exposed to the various humidity environments by placing the PXRD aluminum sample holder on a plastic stage raised above the jar bottom. Ambient conditions were achieved by placing the aluminum sample holders in a covered petri dish exposed to the atmosphere in the laboratory.

To conduct a spontaneous cocrystallization experiment, cofomers were weighed out in an stoichiometric ratio of either 2:1 or 1:1 (API:diacid), as determined by the product cocrystal and consistent with the ratios reported in the literature. The cofomers were milled separately for 25 min at 25 Hz and sifted to select the 45–90 μm grain size fraction. Sifted cofomers were then weighed (to within ± 1 mg) in the appropriate stoichiometric ratio of API:diacid and combined in a 15-mL glass sample vial to a total of at least 500 mg mixture. This mixture of powders in the vial was stirred vigorously by a vortexer for 2 min, then sifted three times through a stack of 40- 60- and 80-mesh sieves to achieve optimal mixing of powders without mechanical crushing. Aliquots of the mixture were immediately packed into

aluminum PXRD sample holders and scanned by PXRD for the first time point. Each sample holder contained approximately 100 mg of sample in a well cavity with a depth of 1 mm. The samples were then placed in their humidity exposure chambers and only removed for 15 min at a time for periodic data collection. An average experiment involved collection of 6–8 traces for each sample over several weeks. An explanation of the method for extracting cofomer and cocrystal signal from the PXRD traces and generating the resultant growth curves are given in the Supplementary Information.

Results and Discussion

We note at the outset that all the systems studied here form cocrystal spontaneously to some extent when input powders are mixed and left to stand. The study of solid-state cocrystallization reactions is in its infancy. Lacking a faithful kinetic model for the process, we are unable to report rate constants, and thus we base our observations on empirical growth curves derived from PXRD traces of cocrystallizing mixtures taken at various time points. A PXRD data set of a 2:1 mixture of caffeine and malonic acid, respectively, subjected to a 50% RH environment, is shown in Fig. 3. The physical mixture of the two cofomers, manifested as two superimposed PXRD traces at the first time point (0 h), is seen to give way monotonically to the cocrystal trace. Two non-overlapping peaks in the PXRD traces, one from a cofomer and one from the cocrystal, are singled out to track the fraction of cocrystal present in the mixture. The 2θ values of these peaks for each cocrystal system are given in Table S1. Growth curves for the caffeine-malonic acid cocrystal, CA:MA (2:1), at four humidity levels are shown in Fig. 4. Within experimental error, cocrystal is formed irreversibly at all humidity levels.

Two trends emerge when comparing cocrystallization data across all systems. The first and more robust trend is that of humidity's effect on cocrystallization. As we found

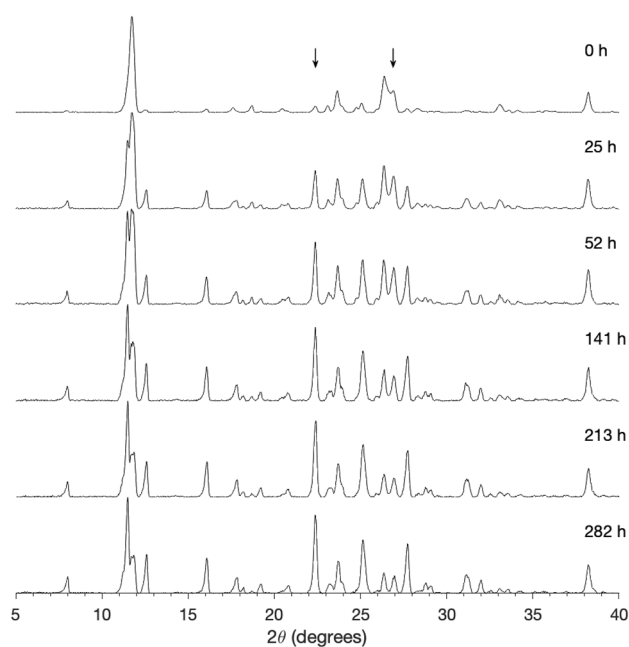


Fig. 3 PXRD traces of a 2:1 mixture of caffeine and malonic acid subjected to 50% relative humidity. The panels show the spontaneous emergence of CA:MA (2:1) cocrystal over nearly 12 days. By 282 h, the formation of cocrystal is over 80% complete, as shown in Fig. 4. The time points are given in the upper right of each panel in hours. The arrow at $2\theta = 27.06^\circ$ indicates the peaks used to monitor the disappearance of a coformer (caffeine), and the arrow at $2\theta = 22.46^\circ$ is used to monitor the emergence of cocrystal. Distinct, non-overlapping peaks, such as these, are used to generate growth curves. Reference PXRD traces of caffeine, malonic acid, and the cocrystal are given in Figure S3

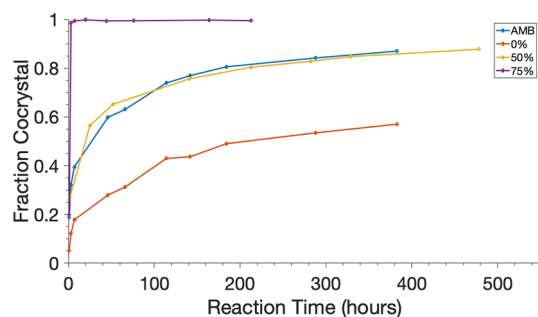


Fig. 4 Growth curves for the formation of caffeine and malonic acid cocrystal, CA:MA (2:1). Each data point was generated using PXRD from a sample exposed to the associated humidity in the legend (upper right). The fraction of signal corresponding to cocrystal is plotted on the vertical axis. The sample exposed to 75% RH shows fast, quantitative conversion. Samples kept at ambient conditions and exposed to 50% RH show nearly the same rate of conversion to cocrystal. This figure is repeated as Figure S4 in the Supplementary Information

in our detailed studies of the CA:MA (2:1) cocrystal system, solvent vapors can dramatically catalyze the cocrystallization process [14, 25]. For each cocrystal system, without exception, samples exposed to 75% RH experienced the most rapid and complete conversion from starting material to cocrystal. Conversely, samples held in desiccant chambers experienced little to no cocrystal conversion when tracked over an equivalent time period. Samples at ambient conditions and 50% RH consistently achieved comparable rate and extent of cocrystallization, and in some cases their growth curves crossed. Within this established phenomenon of solvent vapor digestion, a few cocrystals displayed notable deviations from the trend. The NA:MA (2:1) system did not appear to produce any cocrystal at ambient conditions despite achieving almost 50% conversion at 50% RH. This experiment was repeated at ambient conditions by the same procedure, and it yielded the same result. The NA:SU (2:1) system displayed an irregularity at 50% RH, where the 50% RH experiment more closely matched the desiccant chamber (0% RH) data than it did data from the experiment run at ambient conditions. The TH:GA (1:1) and CA:ME (2:1) systems both appear to produce cocrystal at 75% RH, but data at other levels of humidity indicate negligible cocrystallization. This result suggests that some systems may spontaneously form cocrystal only above a solvent vapor pressure threshold, which in itself may constitute an important clue to the molecular mechanism.

The second trend we observe is that of the rate and extent of cocrystallization with respect to the coformers themselves. Excepting oxalic acid, the prevailing trend with respect to coformers is that longer chain diacids exhibit lower rate and extent of cocrystallization. In the case of caffeine, CA:MA (2:1) cocrystal formed more rapidly and to a greater extent than did CA:ME (1:1), which in turn was more rapid than CA:ME (2:1) and CA:GA (2:1). The CA:ME (2:1) system is comparable to CA:GA (2:1) at 75% RH. At lower humidity levels, CA:ME (2:1) shows only small conversion to cocrystal, thus limiting any comparisons between these two systems at lower humidity levels. The theophylline systems exhibit the same trend with respect to malonic acid, maleic acid, and glutaric acid. One notable difference is that each diacid cocrystallized with theophylline to a greater extent over the same period of time when compared to reaction with caffeine. Nicotinamide cocrystals exhibit one exception to this trend in NA:GA (2:1). The relative rate and extent of cocrystallization with respect to nicotinamide for each coformer is as follows: NA:MA (2:1) > NA:GA (1:1) > NA:FU (1:1) > NA:SU (2:1). Diacids formed cocrystal with nicotinamide at a significantly slower rate and to a lesser extent when compared to their counterpart reactions with caffeine and theophylline. The comparison of nicotinamide cocrystals to caffeine and theophylline cocrystals is made difficult by the lack of NA:ME cocrystal and the inability for caffeine

and theophylline to cocrystallize with fumaric and succinic acids. These discrepancies may be attributable to the significant difference in chemical structure of nicotinamide when compared to the other two APIs. Both caffeine and theophylline are fused-ring structures, differing by a single methyl group, while nicotinamide is a monocyclic compound on a pyridine scaffold with one amide functional group (Fig. 1). These structural differences lead to different synthons in the cocrystal. With the exception of glutaric acid in the case of nicotinamide, all diacids follow the same trend: shorter-chain diacids form cocrystal faster.

Oxalic acid is the only cofomer to buck the trend in diacid chain length. Oxalic acid lacks methylene or methine groups between its carbonyl carbons, restricting its intramolecular torsion to a single dihedral angle between the two carboxyl groups. This decreased conformational flexibility relative to other diacids may belie the lower rate of cocrystallization with APIs relative to malonic acid. Further kinetics studies will be needed to confirm the interplay between internal torsional degrees of freedom and alkyl chain length in cocrystallization.

Additional features in the data are worth noting. Some cocrystal systems studied here show rapid cocrystallization upon initial mixing. This is evident in the first data point in many growth curves, taken soon after mixing the input powders. Systems such as CA:MA (2:1), TH:MA (1:1), TH:ME (1:1), TH:GA (1:1), and NA:MA (2:1) show 10–30% conversion at the first data point, while other systems show no detectable signs of conversion in the early stages. Rapid formation of cocrystal at the outset does not appear to correlate with later conversion. For example, TH:GA (1:1) forms cocrystal quickly at 0% RH, 50% RH, and ambient conditions, but it shows no additional conversion beyond the initial amount, while at 75% RH, cocrystal continues to form, leading to nearly 90% conversion at 200 h. A similar pattern is seen in the TH:ME (1:1) system. Some of the variation we observe in cocrystal formation is likely due to imperfect mixing of the crystallites of the input materials, leading to pockets of crystallites of one material surrounded by the other material. While we have taken measures to ensure thorough mixing of powders, there is no guarantee of perfect mixing at the crystallite level. The data suggest that crystallites must come into physical contact to initiate spatial diffusion, which eventually leads to cocrystal formation. Imperfect mixing at the crystallite level will necessarily attenuate cocrystal formation.

In virtually all data sets, cocrystal formation is markedly slower at 0% RH compared with other humidity levels. While ambient conditions fluctuate with the local weather, they are closest to 50% RH overall, and growth curves for the two track in most cases within experimental error. Many systems, however—CA:ME (1:1), CA:ME (2:1), TH:OX (2:1), TH:ME (1:1), TH:GA (1:1), NA:FU (1:1), NA:SU

(2:1)—show a dramatically faster and greater extent of cocrystal formation at 75% RH compared with other humidity levels used in our study. We intentionally did not use humidity levels greater than 75% RH, in order to avoid deliquescent conditions, which are known to induce alternate pathways to cocrystal formation—namely, dissolution and recrystallization from solvent droplets [33]. In some cases, such as CA:MA (2:1), CA:ME (1:1), CA:ME (2:1), TH:OX (2:1), TH:ME (1:1), TH:GA (1:1), NA:FU (1:1), and TH:SU (2:1), the data suggest a threshold level of humidity, above which cocrystal forms much faster. There does not appear to be any obvious pattern to this behavior. This observation further underscores what has already been reported about vapor-catalyzed reactions in the solid state, and it further underscores the need for its molecular mechanism. It also provides important clues about vapor catalysis of solid-state cocrystallization reactions, and it leaves open the possibility that there may not be a universal mechanism of molecular transport for all systems that is consistent with the data presented here.

Conclusion

Results from experiments reported herein demonstrate the acceleration effect of humidity on spontaneous cocrystallization in 14 different cocrystal systems. Comparison across cocrystal systems indicates that cofomer structure plays an important role in the rate at which cocrystal is formed, with longer-chain diacids tending toward a slower reaction rate. We have also identified several cocrystals beyond CA:MA (2:1) that react quickly and reach near-quantitative conversion: TH:MA (1:1), TH:ME (1:1), and NA:MA (2:1) all achieve > 90% conversion to cocrystal within two weeks at 75% RH, making them strong candidates for further study. We have intentionally chosen systems that are free of hydrates, although the issue of hydrates and hygroscopicity warrants a follow-up study such as this one [18, 19, 21]. Investigations of the systems in this study by microscopy and solid-state NMR are ongoing in our laboratory. It is worth noting that malonic acid reacts quickly and quantitatively with all three APIs in our study (caffeine, theophylline, and nicotinamide), which raises intriguing questions linking its structural features with its reactive nature. The fact that all cocrystals in our study exhibit spontaneous cocrystallization to some extent has consequences for their thermodynamic and kinetic stability relative to the input materials [34]. Work is underway in our laboratory to make fundamental thermodynamic measurements on cocrystals.

Supplementary Information The online version contains supplementary material available at <https://doi.org/10.1007/s10870-022-00922-8>.

Acknowledgements We thank Mr. William Mohler and Mr. Michael Miller of Oberlin College for their assistance at various stages of this project.

Funding Funding for this research was provided by National Science Foundation, RUI (Awards CHE-1464948 and CHE-2100582); National Science Foundation, MRI (Award DMR-0922588). Support is also acknowledged from Oberlin College.

Declarations

Conflict of interest The authors have no conflict of interest to declare that are relevant to the content of this article.

References

- Karimi-Jafari M, Padrela L, Walker GM, Croker DM (2018) Creating cocrystals: a review of pharmaceutical cocrystal preparation routes and applications. *Cryst Growth Des* 18:6370–6387
- Steed JW (2013) The role of co-crystals in pharmaceutical design. *Trend Pharm Sci* 34:185–193
- Blagden N, Berry DJ, Parkin A, Javed H, Ibrahim A, Gavan PT, De Matos LL, Seaton CC (2008) Current directions in co-crystal growth. *New J Chem* 32:1659–1672
- Sarceviča I, Orola L, Nartowski KP, Khimyak YZ, Round AN, Fábíán L (2015) Mechanistic and kinetic insight into spontaneous cocrystallization of isoniazid and benzoic acid. *Mol Pharmaceutics* 12:2981–2992
- Stoler E, Warner JC (2015) Non-covalent derivatives: cocrystals and eutectics. *Molecules* 20:14833–14848
- Fernandes J, Sardo M, Mafra L, Choquesillo-Lazarte D, Massiocchi N (2015) X-Ray and NMR crystallography studies of novel theophylline cocrystals prepared by liquid assisted grinding. *Cryst Growth Des* 15:2674–2683
- Kaupp G (2008) Waste-free synthesis and production all across chemistry with the benefit of self-assembled crystal packings. *Phys Org Chem* 21:630–643
- Wieczorek-Ciurowa K (2007) Mechanochemical syntheses as an example of green processes. *J Therm Anal Cal* 88:213–217
- Report on the Environment: Volatile Organic Compounds; Environmental Protection Agency. U.S. EPA, 2018b.
- 2014 National Emissions Inventory, version 2. U.S. Environmental Protection Agency. U.S. EPA, 2018b.
- Howard JL, Cao Q, Browne DL (2018) Mechanochemistry as an emerging tool for molecular synthesis: what can it offer? *Chem Sci* 9:3080–3094
- Tumanova N, Tumanov N, Robeyns K, Fischer F, Fusaro L, Morelle F, Ban V, Hautier G, Filinchuk Y, Wouters J, Leyssens T, Emmerling F (2018) Opening Pandora's Box: chirality, polymorphism, and stoichiometric diversity in flurbiprofen/proline cocrystals. *Cryst Growth Des* 18:954–961
- Kuroda R, Higashiguchi K, Hasebe S, Imai Y (2004) Crystal to crystal transformation in the solid state. *CrystEngComm* 6:463–468
- Ji C, Hoffman MC, Mehta MA (2017) Catalytic effect of solvent vapors on the spontaneous formation of caffeine-malonic acid cocrystal. *Cryst Growth Des* 17:1456–1459
- Ibrahim AY, Forbes RT, Blagden N (2011) Spontaneous crystal growth of co-crystals: the contribution of particles size reduction and convection mixing of the co-formers. *CrystEngComm* 13:1141–1152
- Maheshwari C, Jayanskar A, Khan N, Amidon G, Rodriguez-Hornedo N (2009) Factors that influence the spontaneous formation of pharmaceutical cocrystals by simply mixing solid reactants. *CrystEngComm* 11:493–500
- Braga D, Giuffreda SL, Rubini K, Grepioni F, Chierotti MR, Gobetto R (2007) Making crystals from crystals: three solvent-free routes to the hydrogen bonded co-crystal between 1,1'-di-pyridylferrocene and anthranilic acid. *CrystEngComm* 9:39–45
- Good D, Miranda C, Rodriguez-Hornedo N (2011) Dependence of cocrystal formation and thermodynamic stability on moisture sorption by amorphous polymer. *CrystEngComm* 13:1181–1189
- Veith H, Zaeh M, Luebbert C, Rodriguez-Hornedo N, Sadowski G (2021) Stability of pharmaceutical co-crystals at humid conditions can be predicted. *Pharmaceutics* 13:433
- Veith H, Luebbert C, Rodriguez-Hornedo N, Sadowski G (2021) Co-Crystal screening by vapor sorption of organic solvents. *Cryst Growth Des* 21:4445–4455
- Thakur TS, Thakuria R (2020) Crystalline multicomponent solids: an alternative for addressing the hygroscopicity issue in pharmaceutical materials. *Cryst Growth Des* 20:6245–6265
- Sarceviča I, Orola L, Belyakov S, Veidis M (2013) Spontaneous cocrystal hydrate formation in the solid state: crystal structure aspects and kinetics. *New J Chem* 37:2978–2982
- Friščić T, Jones W (2009) Recent advances in understanding the mechanism of cocrystal formation via grinding. *Cryst Growth Des* 9:1621–1637
- Užarević K, Halasz I, Friščić T (2015) Real-time and in situ monitoring of mechanochemical reactions: a new playground for all chemists. *J Phys Chem Lett* 6:4129–4140
- Mandala VS, Loewus SJ, Mehta MA (2014) Monitoring cocrystal formation via in situ solid-state NMR. *J Phys Chem Lett* 5:3340–3344
- Lukin S, Lončarić I, Tireli M, Stolar T, Blanco MV, Lazić P, Užarević K, Halasz I (2018) Experimental and theoretical study of selectivity in mechanochemical cocrystallization of nicotinamide with anthranilic and salicylic acid. *Cryst Growth Des* 18:1539–1547
- Trask AV, Motherwell WDS, Jones W (2005) Pharmaceutical cocrystallization: engineering a remedy for caffeine hydration. *Cryst Growth Des* 5:1013–1021
- Trask AV, Motherwell WDS, Jones W (2006) Physical stability enhancement of theophylline via cocrystallization. *Int J Pharm* 320:114–123
- Hathwar VR, Pal R, Row TNG (2010) Charge density analysis of crystals of nicotinamide with salicylic acid and oxalic acid: an insight into the salt to cocrystal continuum. *Cryst Growth Des* 10:3306–3310
- Karki S, Friščić T, Jones W (2009) Control and interconversion of cocrystal stoichiometry in grinding: stepwise mechanism for the formation of a hydrogen-bonded cocrystal. *CrystEngComm* 11:470–481
- Orola L, Veidis MV (2009) Nicotinamide fumaric acid supramolecular cocrystals: diversity of stoichiometry. *CrystEngComm* 11:415–417
- Thompson LJ, Voguri RS, Cowell A, Male L, Tremayne M (2010) The cocrystal nicotinamide-succinic acid (2/1). *Acta Crystallogr Sect C* 66:o421–o424
- Jayanskar A, Good DJ, Rodriguez-Hornedo N (2007) Mechanisms by which moisture generates cocrystals. *Mol Pharm* 4:360–372
- Ervasti T, Aaltonen J, Ketolainen J (2015) Theophylline-nicotinamide cocrystal formation in physical mixture during storage. *Int J Pharm* 486:121–130

Publisher's Note Springer Nature remains neutral with regard to jurisdictional claims in published maps and institutional affiliations.